Brace root phenotypes predict root lodging susceptibility and the contribution to anchorage in maize

Authors: Ashley N. Hostetler[1], Lindsay Erndwein[1], Jonathan W. Reneau[1], William Cantera[2], Adam Stager[1,3], Herbert G. Tanner[3], Douglas Cook[4], Erin E. Sparks[1]

Affiliations:
[1]Department of Plant and Soil Sciences and the Delaware Biotechnology Institute, University of Delaware, Newark, DE
[2]Department of Engineering Computer & Information Sciences, University of Delaware, Newark, DE
[3]Department of Mechanical Engineering, University of Delaware, Newark, DE
[4]Department of Mechanical Engineering, Brigham Young University, Provo, UT

Contact information for corresponding author: Erin E. Sparks esparks@udel.edu

Author email addresses: ahende@udel.edu, erndwein@udel.edu, jreneau@udel.edu, wcantera@udel.edu, astager@udel.edu, btanner@udel.edu, d.cook@byu.edu, esparks@udel.edu

Abstract

A changing global climate brings increasingly prevalent and severe storms that threaten crop production by imparting mechanical stresses. Plant failure due to mechanical stress is termed lodging and in the United States, yield loss due to lodging has been estimated at 7-25% for maize (*Zea mays*). In maize, the presence of specialized aerial brace roots has been shown to increase anchorage and root lodging resistance. However, beyond scoring for presence, there have been limited attempts to define the brace root phenotypes that optimize anchorage. This study reports variable root lodging and plant biomechanics in a population of 52 maize inbred lines. To quantify the variation in brace root phenotypes within this population, a semi-automated phenotyping workflow was developed. These empirical measurements were integrated into predictive random forest models to demonstrate that brace root phenotypes can classify root lodging incidence and plant biomechanics. The prediction accuracy of these models is driven by multiple brace root phenotypes suggesting that anchorage can be optimized by the manipulation of multiple functional traits. Plant height has been previously associated with lodging susceptibility yet the inclusion of plant height as a predictor does not always improve prediction accuracy. Previously, brace root node number has been shown to be genetically linked to plant height and here we show that additional brace root phenotypes are linked to plant height but with opposing effects on root lodging susceptibility. Together these data define the important brace root phenotypes that predict root lodging resistance and demonstrate the need to uncouple the linkage between plant height and root traits for the development of climate resilient crops.

Introduction

A changing global climate is increasing the severity and prevalence of storm systems, which threatens crop production. Crop failure from mechanical stress is called lodging and is defined as the displacement of plants from vertical (Rajkumara, 2008). In maize, lodging is reported to cause between 7-25% yield loss (Carter and Hudelson, 1988; Flint-Garcia et al., 2003; Tirado et al., 2020) and can be attributed to stalk and/or root failure (Berry et al., 2004; Rajkumara, 2008). Stalk lodging occurs at late growth stages when internodes buckle below the ear, whereas root lodging can occur at any growth stage when the root system fails by uprooting and/or breaking (Berry et al., 2004; Rajkumara, 2008; Erndwein et al., 2020; Hostetler et al., 2021). The development of lodging-resistant crops relies on a detailed understanding of the underlying factors that contribute to lodging susceptibility. However, defining these factors has been limited by the reliance on unpredictable weather patterns to induce natural lodging events. To overcome this limitation, measures of plant anchorage have been developed as a proxy for root lodging (Erndwein et al., 2020). Using both natural lodging events and measures of plant anchorage, several factors that impact lodging have been defined, and include field management practices, plant stage at lodging, plant genotype, and plant architecture (e.g. root system architecture and plant height) (Carter and Hudelson, 1988; Berry et al., 2004; Rajkumara, 2008).

In maize, the primary plant architecture that has been linked to root lodging resistance and anchorage is the size and extent of the root system (Thompson, 1972; Sanguineti et al., 1998; Liu et al., 2012; Farkhari et al., 2013; Sharma and Carena, 2016; Shi et al., 2019). Within the root system, the presence of aerial nodal roots, called brace roots, are consistently associated with the ability to resist root lodging (Hoppe et al., 1986; Carter and Hudelson, 1988; Stamp and Kiel, 1992; Liu et al., 2012; Sharma and Carena, 2016; Shi et al., 2019; Blizard and Sparks, 2020; Hostetler et al., 2021). Beyond quantifying the presence of brace roots, there have been limited studies that quantify other brace root phenotypes that contribute to root lodging resistance and anchorage. A handful of studies have identified the number of brace root whorls in the ground (Liu et al., 2012; Sharma and Carena, 2016; Shi et al., 2019; Reneau et al., 2020), the number of brace roots in a whorl (Liu et al., 2012; Sharma and Carena, 2016), the brace root diameter (Liu et al., 2012; Sharma and Carena, 2016), and the brace root spread width (Sharma and Carena, 2016) as important phenotypes for root lodging resistance. In other crops, plant height is a known factor in lodging susceptibility, however, studies in maize that report a link between plant height and root lodging have been variable. One study showed no correlation between plant height and root lodging in a natural root lodging event (Sharma and Carena, 2016), whereas another study showed plant height as a secondary factor in root lodging models, which were validated by natural root lodging events (Brune et al., 2018). The wide-spread interpretation of these results has been limited by a small number of genotypes per study, disparate phenotypes analyzed in each study, and a primary reliance on univariate correlations. Therefore, a detailed assessment of phenotypes at the population level is required to define how plant architectures contribute to root lodging resistance and anchorage.

In this study, a population of 52 maize inbred lines was assessed for root lodging after a natural storm event and by quantifying the brace root contribution to anchorage in the absence of lodging. Within this population, there was substantial variation in root lodging susceptibility, root lodging severity, stalk flexural stiffness, and the brace root contribution to anchorage. To link brace root phenotypes to root lodging resistance and anchorage necessitates a high throughput brace root

phenotyping workflow. Current root phenotyping methods are either labor intensive, rely on subjective manual data collection, and/or are not targeted for brace root phenotyping (Trachsel et al., 2011; Das et al., 2015; Zhan et al., 2019; Salungyu et al., 2020, Sanguineti et al., 1998; Liu et al., 2012; Sharma and Carena, 2016). Thus, we developed a workflow that non-destructively captures RGB (Red Green Blue) images using a ground-based robot and extracts brace root phenotypes through a semi-automated root tagging pipeline. These phenotypes were paired with manually acquired plant height data. Consistent with previous results, individual phenotype correlations with root lodging and anchorage were low. However, when using brace root phenotypes as predictors, machine learning models predicted root lodging and plant anchorage with high accuracy. Multiple brace root phenotypes drove the decision tree, which highlights the importance of multi-trait analyses for understanding the plant architectures that impact lodging susceptibility. Further, the inclusion of plant height as a predictor did not always change the overall model accuracy. Thus, this work demonstrates the linkage between plant height and brace root traits, which have opposing effects on lodging susceptibility.

Materials and Methods

Plant Material

A maize (*Zea mays*) population, consisting of 52 inbred genotypes with genetic and phenotypic diversity (**Table S1**), was grown in the summer of 2018, 2019, and 2020 at our Newark, DE field site (39° 40' N and 75° 45' W) with overhead irrigation. Each year, 2-4 replicate plots (12' single row) of eighteen seeds per plot were planted in a randomized design. Seeds were planted on 5/30/2018, 5/22/2019, and 06/01/2020. Monthly temperature averages, rainfall estimates, and wind averages can be found in **Table S2**. Additional weather data can be found at the Delaware Environmental Observing System (http://www.deos.udel.edu) and selecting the Newark, DE-Ag Farm station. Pre-emergence (Lexar at 3.5 quart per acre and Simazine at 1.2 quart per acre) and post-emergence (Accent at 0.67 ounces per acre) herbicides were applied. Soil insecticide COUNTER 20G was applied at 5.5 lbs per acre at planting. Ammonium Sulfate 21-0-0 was applied at 90 lbs per acre at planting, and 30% Urea Ammonium Nitrate (UAN) was applied at 40 gallons per acre approximately 1-month after planting (at knee high).

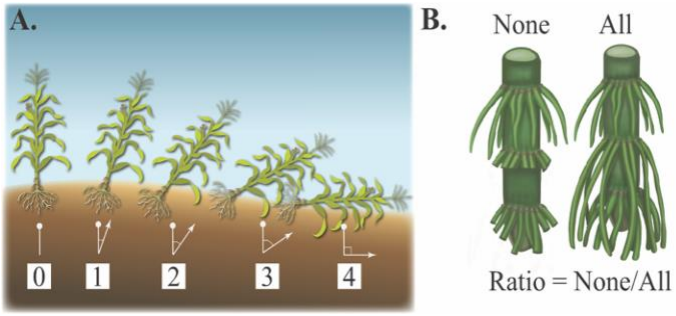

Figure 1. Overview of the methods for quantifying root lodging and the brace root contribution to anchorage. (A) A lodging index score was assigned to each plant according to the degree of displacement and used as a metric for severity. An index score of 0 indicated plants were still vertical (no root lodging), an index score of 1 indicated that plants experienced a 1–30-degree displacement, an index score of 2 indicated plants experienced a 31–60-degree displacement, an index score of 3 indicated plants experienced a 61–80-degree displacement, and an index score of 4 indicated plants were on the ground (90-degree displacement). (B) Force-Deflection was measured when all brace roots were intact (All) and again after excision of all brace roots that entered the ground (None). The None/All ratio was calculated to determine the contribution of brace roots to anchorage.

Lodging Assessment

In the summer of 2020 on August 4th, approximately 65 days after planting (DAP), Tropical Storm Isaias, originally a destructive Category 1 hurricane, caused extensive root lodging throughout the field. The day after the tropical storm, root lodging data was recorded. For each plot, the total

number of plants and total number of lodged plants were recorded. The percent of root lodging per plot was calculated from these data (number of plants lodged/total number of plants×100) and was used as a metric for root lodging susceptibility. A root lodging index score was assigned for each plant, where a 0 indicated no effect (plants vertical), 1 indicated a 1–30-degree displacement, 2 indicated a 31–60-degree displacement, 3 indicated a 61–80-degree displacement, and 4 indicated a 90-degree displacement (plants were completely on the ground) (**Figure 1A**). An average lodging index was calculated per plot and was used as a metric of lodging severity.

Plant Phenotyping

In 2019, brace root images were manually acquired with a digital camera. At 107 DAP, fields were manually cleared of any weeds or debris, including lower stem leaves. A 0.5-inch label, which included plot number, plant number, and an A or B designation to identify each side of the plant (Plot_Plant_A or Plot_Plant_B), was then secured to each stem with clear tape. Images were collected from both sides of 992 plants representing the 52 inbred genotypes. In 2020, brace root images were collected with a ground-based Brace Root phenotyping robot (BRobot). BRobot is a modified Superdroid LT2 Tracked ATR Robot Platform with a custom controller and side mounted FLIR 3.2 MP Color Blackfly camera (**Figure S1**). Plots were marked with an orange stake, and individual plants were marked with a yellow popsicle stick for reference. Only the number of brace root whorls that entered the ground was quantified from these images.

For the 2019 data analysis, we developed a semi-automated root tagging graphical user interface (GUI) to optimize image processing (**Figure S2**). This new workflow enables annotation and analysis on the scale of 1-2 minutes per image. The height of the tag adhered to each plant was used as a scale (pixels per inch) and phenotypes were measured for only the brace root whorls that entered the ground. These phenotypes are measured sequentially as 1) number of brace roots per whorl (where whorl 1 is closest to the ground), 2) single outermost brace root width for the highest whorl in the ground, 3) stalk width, and 4) a right triangle on each side of the plant from the outermost root from highest whorl in the ground. The right triangle is used to extract the height of the whorl on the stalk (*a* leg of a right triangle), the distance from the stalk-to-root grounding (*c* leg of a right triangle), and the root angle (B angle of the right triangle). The brace root spread width was calculated as the sum of the stalk width, and the *b* leg from the triangle on both sides of the plant. The root tagging workflow extracts pixel information and a post processing script converts pixels to inches or degrees. Inches were converted into centimeters for data analysis. Left and right (A and B) phenotyping outputs were compared with a Pearson correlation analysis in R ver. 4.0.2 (R Core Team, 2013) with the *corrplot* package ver. 0.84 (Wei and Simko, 2017). A high correlation (r range 0.55-0.79) between A and B images indicates that the root tagging workflow has high precision (**Figure S3**), therefore measurements were summed (root number per whorl) or averaged (all other phenotypes) to provide a per-plant brace root phenotypic profile and reduce the effect of phenotyping error. Plant height was manually measured during reproductive development and defined as the distance from the base of plant to the top of the tassel.

Field Based Measurements of Plant Biomechanics

Non-destructive, field-based measurements of plant biomechanics were collected with the Device for Assessing Resistant to Lodging IN Grains (DARLING) (Cook et al., 2019) as described in Reneau et al., (2020). In 2018, 3-5 plants per plot were tested at 144-165 DAP. In 2019, all viable plants were tested at 118-129 DAP. Plants were tested after dry down to avoid daytime variation

as previously reported (Reneau et al., 2020). Plants were excluded from testing if their root systems were overlapping with neighboring plants, there was disease or pest damage, or plants were damaged during weed control measures. For each test, the pivot point of the device was aligned with the base of the plant, and the load cell was placed in contact with the stalk at 0.64 m. Three cycles of deflection, each displacing the stalk approximately 15-degrees before returning to 0-degrees, were applied to each plant. Output of each test is a .csv file of force-rotation data. Rotation, measured from an inertial measurement unit (IMU), was converted from degrees to radians with the following equation:

$$\theta = deg \times \pi/180$$

where π is taken as 3.1415. The rotation in radians was then converted into deflection (δ) with the following equation:

$$\delta = h \times sin\theta$$

where h is the height of the applied load (0.64 m) and θ is the rotational angle (radians). The slope of the Force-Deflection data (N/m) was determined by fitting a line to the entire dataset (loading and unloading data for all three cycles). We previously determined that this data extraction method is reliable and comparable to extracting the slope of just the loading data (Reneau et al., 2020).

Flexural stiffness, which is a property of the stalk and assumes the plant acts as a cantilever beam with a rigid attachment at the base, was calculated for measurements of plants with all brace roots intact. Flexural stiffness (Nm^2) is represented as the product of the Young's Modulus (E) and the second moment of inertia (I) and is calculated as:

$$EI = \varphi \times \frac{h^3}{3}$$

where φ is the slope of the Force-Deflection data (N/m), and h is the height of the applied load (0.64 m).

To determine the relative contribution of brace roots to anchorage, all brace roots entering the ground were manually excised with pruning shears and Force-Deflection was remeasured in the absence of brace roots. The relative contribution of brace roots was calculated as the ratio between the slope of the Force-Deflection curve with all brace roots removed (None), and the slope of the Force-Deflection curve with all brace roots intact (Ratio=None/All; **Figure 1B**). We have previously shown that repeat testing does not alter the slope of the Force-Deflection curve and any changes in Force-Deflection are due to the removal of brace roots (Reneau et al., 2020). Thus, a higher ratio is indicative of a lower contribution of brace roots to anchorage.

Genotype Relatedness

The phylogenetic relationship among genotypes was determined using PAUP* version 4.0a169 and SVDquartets (Chifman and Kubatko, 2014, 2015; Wascher and Kubatko, 2021). A species tree was generated with exon data, which was downloaded for 41 of the 52 inbred genotypes from the SNPVersity database on MaizeGDB. The exon data downloaded was aligned to the B73 reference genome ver. 2. In instances where a single genotype was represented more than once, all data sets were retained. When the genotype data clustered together, a taxon-partition was used to assign both sets of sequence data to a terminal branch. When genotype data did not cluster, both sets of sequence data were retained as individual branches. The phylogenetic relationships can be visualized in **Figure S4**.

Heritability Calculations

Broad-sense heritability (H^2) was calculated in R ver. 4.0.2 (R Core Team, 2013) with the following equation:

$$H^2=\sigma^2_G/(\sigma^2_G + \sigma^2_E)$$

where σ^2_G is the genotypic variance and σ^2_E is the experimental error variance (Holland et al., 2002). H^2 was calculated for 2020 root lodging data (susceptibility and severity), 2019 phenotype data, and 2018/2019 biomechanical data to determine the proportion of phenotypic variance that is due to the underlying genetics.

Statistical Analyses

All statistical analyses were performed using R ver. 4.0.2 (R Core Team, 2013). An analysis of variance (ANOVA) was performed to determine if there were significant differences among genotypes for each of the phenotypes. Further, a two-way ANOVA was performed to determine the genotype and year effect on stalk flexural stiffness and the None/All ratio. Prior to running each ANOVA, a Shapiro-Wilk test was used to determine if data was normally distributed. If data deviated from a normal distribution ($p<0.05$), a Tukey's Ladder of Powers from the *rcompanion* package ver. 2.3.26 (Mangiafico, 2021) was used to transform the data. Following each ANOVA, if a significant difference was observed, a post-hoc Tukey Honest Significant Difference (HSD) test was performed to test all pairwise comparisons. A principal component analysis (PCA) was used to identify phenotypes that explained the most variability among the genotypes. The PCA was visualized with the *factoextra* package ver. 1.0.7 (Kassambara and Mundt, 2020) in R. Pearson correlation analyses were run on: 1) individual plant paired phenotype and mechanical phenotype data, 2) genotypic phenotype, mechanical phenotype, and root lodging data, and 3) genotypic mechanical phenotype and root lodging data, with the *corrplot* package ver. 0.84. All graphs were generated in R ver. 4.0.2 (R Core Team, 2013) with the *ggplot2* package ver. 3.3.3 (Wickham, 2016).

Predictive Modeling

Machine learning approaches were used to determine if brace root phenotypes could accurately predict root lodging (susceptibility and severity) and mechanical phenotypes (stalk flexural stiffness and the None/All ratio). In R ver. 4.0.2 (R Core Team, 2013) the following packages were used for modeling: *tidyverse* ver. 1.3.0 (Wickham et al., 2019), *tidymodels* ver. 0.1.2 (Kuhn and Wickham, 2020), *ranger* ver. 0.12.1 (Wright and Ziegler, 2017), and *kknn* ver. 1.3.1 (Schliep et al., 2016). For each of the models, data was split into a 90% training set and 10% testing set with a 5-fold cross validation strategy.

A multiple regression model was built using individual plant brace root phenotyping data to predict genotype-averages of root lodging susceptibility. Additionally, genotypes were grouped for categorical classification. For each of the four outcomes (root lodging susceptibility, root lodging severity, stalk flexural stiffness, and the None/All ratio), data were first scaled and centered before classified into one of three groups - low, average, high. For each outcome, genotypes were classified as low when they were less than 1 standard deviation below the mean, genotypes were classified as high when they were greater than 1 standard deviation above the mean, and genotypes were classified as average when they were within +/- 1 standard deviation of the mean. This method was repeated for within-year paired measurements for individual plant classification.

For each outcome, a random forest approach was used with 100 trees. The average accuracy and Receiver Operating Characteristic (ROC) Area Under the Curve (AUC) was extracted for each model. Phenotypes with the highest mean decrease in Gini were considered the most important predictors of the model (Menze et al., 2009). All phenotypes were included as predictors for each of the models. Additional predictors of height and mechanical phenotypes were included in selected models.

Data Availability

All raw data, processed data, and scripts to analyze data are available on GitHub: https://github.com/EESparksLab/Hostetler_et_al_2021

Results

Genotype determines root lodging susceptibility

Although root lodging is prevalent in agricultural cropping systems, it is rarely quantified in the scientific literature. In 2020, a natural lodging event occurred at the Newark, DE field during the late-vegetative and early reproductive growth stages (65 DAP) after brace roots had entered the ground (**Figure S5**). Tropical Storm Isaias brought heavy rains followed by sustained winds that averaged 23.8 miles per hour (mph) with gusts up to 59 mph (**Table S3**). This storm caused extensive root lodging, thus allowing for a detailed assessment of root lodging susceptibility and severity. Although winds were from the West and North West, root lodging was not influenced by field position relative to the wind (**Figure S6**).

For 52 inbred genotypes there was a continuous distribution of root lodging susceptibility and severity, with 826 plants remaining upright while 421 plants root-lodged (**Figure 2A**). For the 421 root-lodged plants there was a distribution of root lodging severity as determined by the degree displacement (**Figure 1A; 2B**). A genotypic-level quantification identified 16 root lodging resistant genotypes, with no root lodging in either plot replicate (**Figure 2C**). There were 36 genotypes that showed variation root lodging in both plot replicates (**Figure 2D**). The broad sense heritability (H^2) estimate of root lodging susceptibility was 0.58 (**Table S4**), however, the phylogenetic relationship of genotypes showed that root lodging resistance is independent of subpopulation classification (**Figure S4**). Together, these data are consistent with genotype-specific, but not subpopulation specific, regulation of root lodging susceptibility. These data further demonstrate that variation in root lodging susceptibility still exists within current maize germplasm resources.

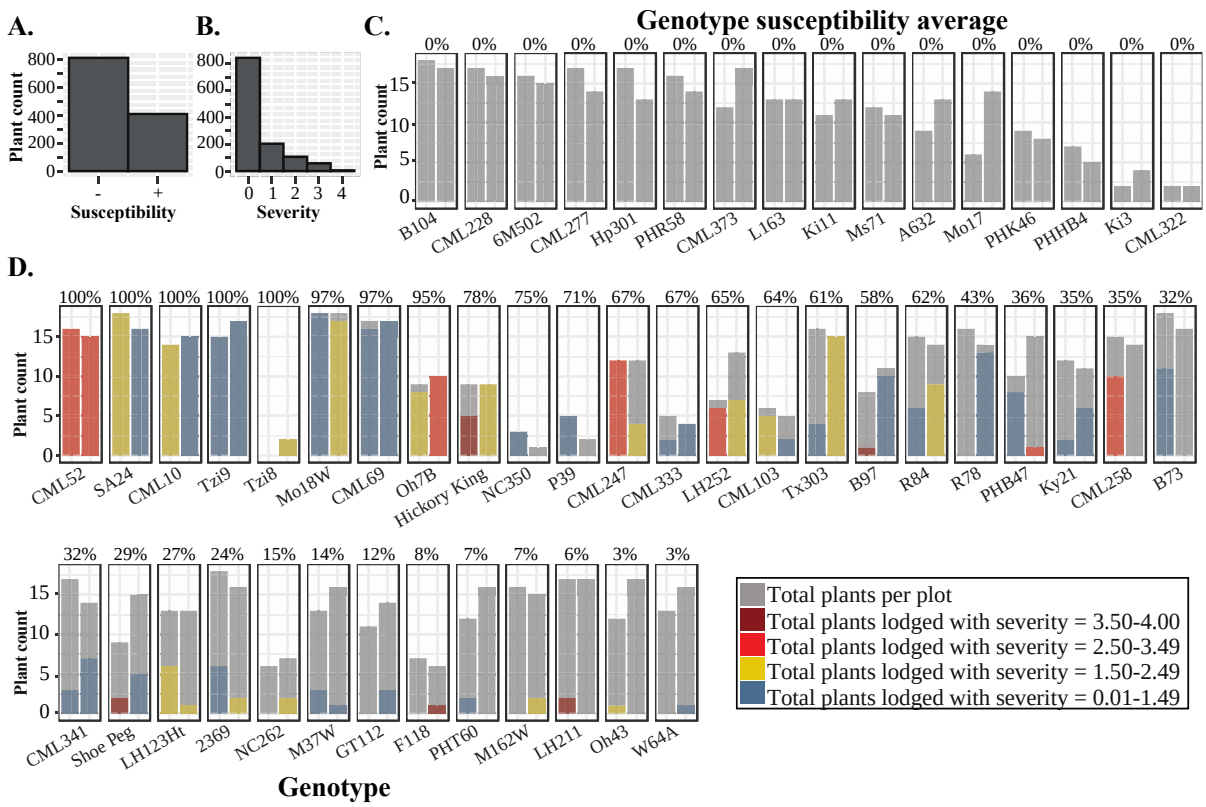

Figure 2. Root lodging varied across 52 maize genotypes. (A) Following Tropical Storm Isaias, 826 plants remained vertical (-) and 421 plants experienced root lodging (+). (B) Of the plants that experienced root lodging, the severity of root lodging varied. (C-D) Each bar represents one replicate plot; gray bars indicate the total number of plants per plot; colored bars indicate the total number of plants that lodged per plot; the genotype susceptibility average (shown at the top of both plots) was defined as 'the total number of plants lodged per genotype/the total number of plants per genotype×100'; the color of the bar represents the average plot severity. (C) There were 16 genotypes that did not root lodge in either plot replicate. (D) There were 36 genotypes that showed variable degrees of root lodging in both plot replicates.

Brace root phenotypes vary between genotypes

We hypothesized that the genotype-specific regulation of root lodging susceptibility is due to the underlying variation in brace root phenotypes within this population. To quantify brace root phenotypes in the absence of root lodging, we developed a semi-automated root tagging workflow (**Figure S2**) that extracts various brace root phenotypes from RGB images (**Figure 3A; Table S5**). Manual quantification of brace root whorl number and plant height were also included in the phenotypic assessment.

All phenotypes varied significantly by genotype (**Figures S7, Tables S6-S7**), and a Principal Component Analysis (PCA) showed a dense, continuous distribution of plants (**Figure 3B**). The first dimension of the PCA explains 29.15% of the variation and is primarily driven by spread width and the stalk-to-root grounding (**Table S8-S9**). The next 6 dimensions, explain an additional 63.50% of the variation (>90% total variation explained) and are each driven by a single phenotype (**Table S8-S9**). Further, phenotypes that are highly correlated (**Figure S8**) also had eigenvectors that loaded in the same plane in the PCA (**Figure 3B**). For example, the spread width and the stalk-to-root grounding eigenvectors load in the same plane and direction (**Figure 3B**) and are highly positively correlated (r = 0.99; **Figure S8**). There is also a negative correlation between the angle

and root height on stalk (r = -0.61; **Figure S8**) and eigenvectors load in the same plane but opposite directions (**Figure 3B**). This suggests that brace root whorls that attach higher on the stalk have a more acute angle. Consistent with the genetic regulation of these phenotypes, H^2 ranged from 0.23 (number of brace root whorls that enter the ground) to 0.40 (stalk-to-root grounding) (**Table S4**). Thus, these data demonstrate underlying genotype-specific variation in individual brace root phenotypes that may contribute to root lodging.

Brace root phenotypes predict root lodging

While there is variation of brace root phenotypes within this population, there is an overall low correlation of individual phenotypes with root lodging susceptibility or severity (**Table 1**). The highest correlation was between the number of brace root whorls that entered the ground and root lodging susceptibility (r = -0.43). This is consistent with previous studies that have reported this phenotype as important for anchorage (Liu et al., 2012; Sharma and Carena, 2016; Shi et al., 2019; Reneau et al., 2020). However, the overall low correlations demonstrate that individual root phenotypes cannot explain root lodging.

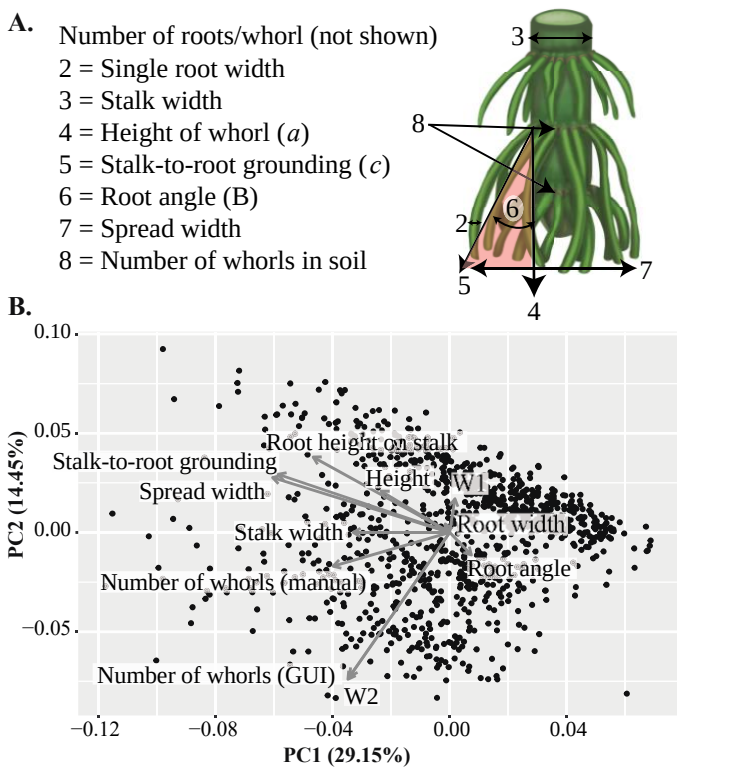

Figure 3. Brace root phenotypes vary among maize genotypes. (A) Brace root phenotypes were quantified with a semi-automated root tagging workflow and phenotypes were only extracted from the brace root whorls that entered the ground. Phenotypes 2, 4, 5, 6, and 8 were extracted for the top-most whorl that entered the ground. The number of roots on each whorl was quantified for all brace root whorls that entered the ground with W1 being the bottom-most whorl (closest to the ground) and W3 being the top-most whorl. The red triangle highlights the right triangle that is used to identify the height of the whorl (*a* leg of the right triangle), the stalk-to-root grounding (*c* leg of the right triangle), and the root angle (B angle of the right triangle). (B) A principal component analysis (PCA) showed a dense, continuous distribution of plants by phenotype, with the first principal component (PC1) explaining 29.15% of the variation and the second principal component (PC2) explaining 14.5% of the variation. PC1 is primarily driven by spread width and the stalk-to-root grounding, whereas PC2 is primarily driven by the number of roots on W2 and the number of whorls that entered the ground.

To further explore the relationship between brace root phenotypes and root lodging, machine learning models were employed. Multiple regression models were used to predict root lodging susceptibility and severity using all GUI-extracted phenotypes and the manual quantification of the number of brace root whorls in the ground as predictor variables. The models were only able to predict root lodging susceptibility with a R^2 value of 0.13 and root lodging severity with a R^2 value of 0.04. It is not surprising that phenotypes measured in one year are unable to predict root lodging for a different year. Consequently, a categorical classification approach was used to determine if brace root phenotypes can predict the relative genotype classification (low, average, high)

for root lodging susceptibility and severity. A random forest model was generated using the same predictor variables as in the multiple regression. From these models, the root lodging susceptibility outcome was predicted with 55.70% accuracy (ROC AUC=0.74), and severity outcome was predicted with 52.60% accuracy (ROC AUC=0.66) (**Table 2**). Thus, brace root phenotypes alone can predict root lodging susceptibility and severity classifications.

Plant height has been historically associated with lodging, as evidenced by the development of dwarf varieties of grain crops during the Green Revolution, which reduced the impact of lodging. The moderate correlations between plant height and lodging susceptibility (r = 0.31) or lodging severity (r = 0.45) in this study suggest that plant height alone cannot not explain root lodging in maize (**Table 1**). To understand the impact of plant height on root lodging in maize, random forest models were run with brace root phenotypes and plant height as predictors. The inclusion of plant height improved the prediction accuracy for root lodging susceptibility (68.0% accuracy, ROC AUC=0.81), but not root lodging severity (55.7% accuracy, ROC AUC=0.76) (**Table 2**). Interestingly, there are low positive correlations between brace root phenotypes and plant height (**Figure S8**), but they have opposing effects on lodging susceptibility (**Table 1**). In other words, taller plants are more likely to root lodge, but taller plants also have larger brace root traits, which limit root lodging. These results support the importance of plant height in the context of brace root phenotypes to limit root lodging.

Brace root phenotypes predict plant biomechanics

Lodging studies rely on unpredictable and erratic weather patterns, making it difficult to design controlled experiments to identify the underlying phenotypic variation influencing root lodging. To overcome these limitations, measurements of plant biomechanics have been used to quantify mechanical phenotypes as a proxy for root lodging resistance (Erndwein et al., 2020). However, the brace root phenotypes that contribute to these mechanical phenotypes are poorly defined. To fill this knowledge gap, stalk flexural stiffness and the contribution of brace roots to anchorage were measured in this population across two field seasons to link brace root phenotypes and mechanical phenotypes.

Stalk mechanical properties were characterized by non-destructive measurements of flexural stiffness using the DARLING (Cook et al., 2019). An analysis of mechanical phenotypes across two field seasons showed that stalk flexural stiffness was impacted by both genotype and year ($p<0.001$, **Figure 4A, Table S10**). However, closer inspection of the genotype by year effect showed that only seven genotypes had variable stalk flexural stiffness between years (**Table S11)**, which is consistent with a H^2 of 0.58 (**Table S4**), suggesting strong genetic control.

The contribution of brace roots to anchorage was defined as the None/All ratio (Reneau et al., 2020; **Figure 1B**). A high ratio (close to 1) shows that brace roots are not impacting plant anchorage, whereas a low ratio (close to 0) shows that plant anchorage is dependent on the brace roots in the ground. Analysis of the None/All ratio across two years shows that the contribution of

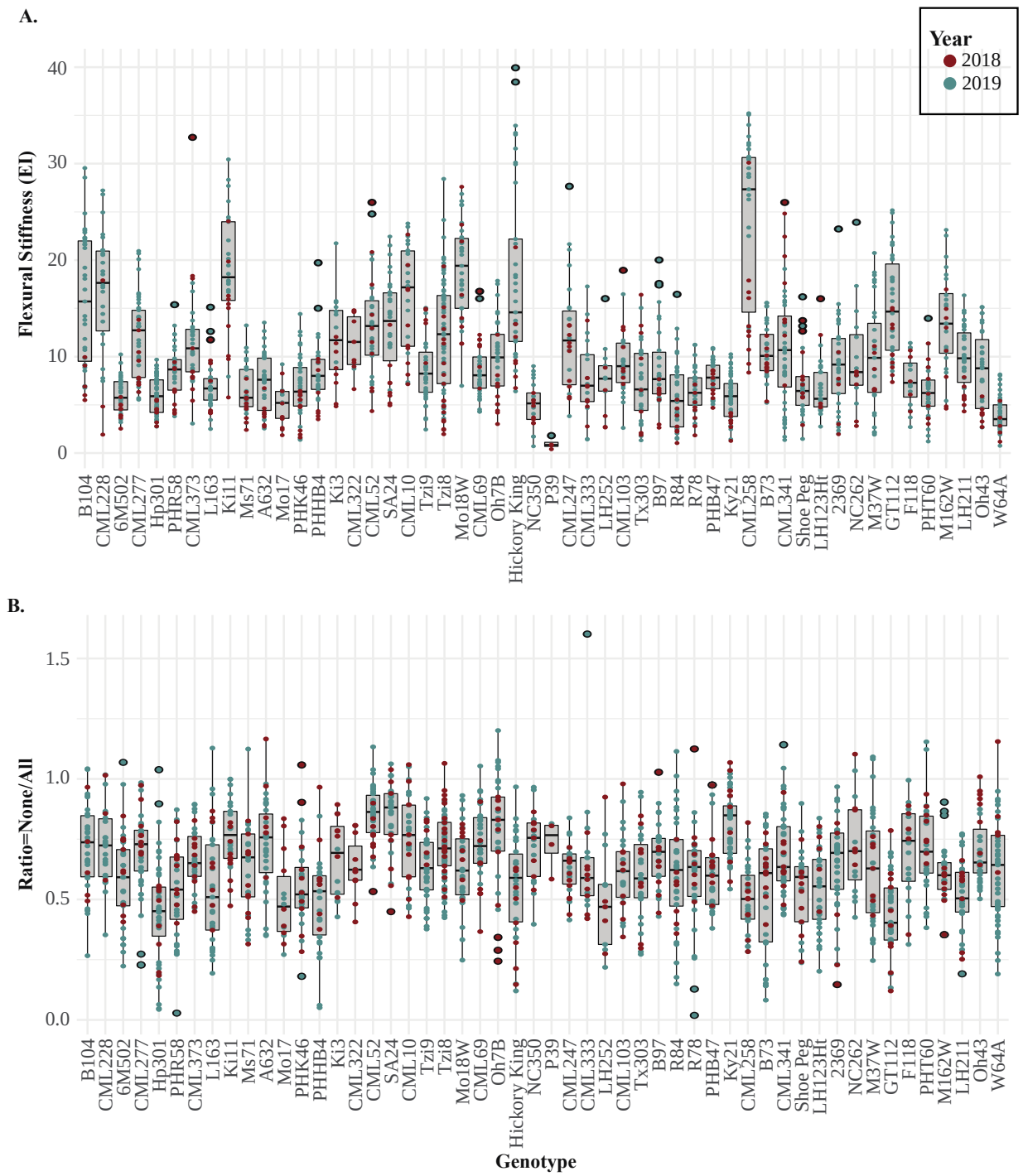

Figure 4. Mechanical phenotypes vary depending on genotype. (A) A two-way analysis of variance (ANOVA) showed that stalk flexural stiffness was impacted by both genotype ($p<0.05$) and year ($p<0.05$). (B) A higher None/All ratio indicates that anchorage was not influenced by brace roots, whereas a lower None/All ratio indicates that brace roots are important in anchorage. A two-way ANOVA showed that the None/All ratio was impacted by genotype ($p<0.05$) but not year ($p>0.05$). (A-B) The color of each dot illustrates which year the data was collected. Outliers are outlined in black. Genotypes are ordered by root lodging classification as in Figure 2.

brace roots to anchorage was only impacted by genotype ($p<0.001$) and not year (**Figure 4B, Table S10**). The H^2 was 0.36 (**Table S4**), which again demonstrates that mechanical phenotypes are under genetic control.

To link brace root phenotypes to mechanical phenotypes, random forest models were again generated; one to predict stalk flexural stiffness and one to predict the None/All ratio. Both models used GUI-extracted phenotypes and the manual quantification of the number of brace root whorls in the ground as predictors. Genotypes were categorized as low, average, or high for each of the outcomes from two-year averages. These models predicted stalk flexural stiffness with 80.40% accuracy (ROC AUC = 0.58), and the None/All ratio with 76.30% accuracy (ROC AUC = 0.79) (**Table 2**). Using one-year paired plant data, instead of two-year genotypic averages, resulted in a decreased prediction accuracy of 75.30% (ROC AUC = 0.82) for the stalk flexural stiffness and 67.00% (ROC AUC = 0.66) for the None/All ratio (**Table 2**). This reduction in accuracy is likely due to the error inherent to each measurement, which is reduced by considering genotypic averages. In contrast to the root lodging predictions, the inclusion of plant height in these models did not dramatically improve the overall prediction accuracy (increase $\leq$ 3%; **Table 2**). Collectively, these data show that brace root phenotypes can predict plant biomechanics, and that brace root phenotypes are better at predicting genotypic-level biomechanics than individual paired plant measurements.

Inclusion of mechanical phenotypes improves the prediction accuracy of root lodging

To determine if the biomechanical measures are a good proxy for root lodging, pairwise Pearson correlations were calculated. Unsurprisingly, there were low correlations between stalk flexural stiffness and root lodging severity ($r = 0.25$) or root lodging susceptibility ($r = 0.14$) (**Figure 5A**), which is consistent with stalk mechanics having a weak link to root anchorage. In contrast, the correlation between the None/All ratio and root lodging susceptibility ($r = 0.36$) or root lodging severity ($r = 0.33$) were moderate (**Figure 5A**). The positive correlations between the None/All ratio and root lodging suggests that the less brace roots contribute to anchorage (e.g., a higher ratio) the greater propensity for root lodging.

To determine if the inclusion of mechanical phenotypes improved the prediction accuracy of the root lodging models (susceptibility and severity), the stalk flexural stiffness and the None/All ratio were included as predictors in the random forest models. With the inclusion of mechanical phenotypes, the prediction accuracies of both root lodging susceptibility and severity were increased by 10.30% and 13.40%, respectively (**Table 2**). However, the addition of plant height to these models resulted in a minimal change in prediction accuracy (+/- 2%), thus suggesting that mechanical phenotypes encompass the contribution of plant height.

Multiple phenotypes equally contribute to the prediction of root lodging and the none/all ratio

To define the phenotypes that optimize plants for root lodging resistance, the predictors that are driving the random forest decision trees in each of the four outcome models were investigated. For

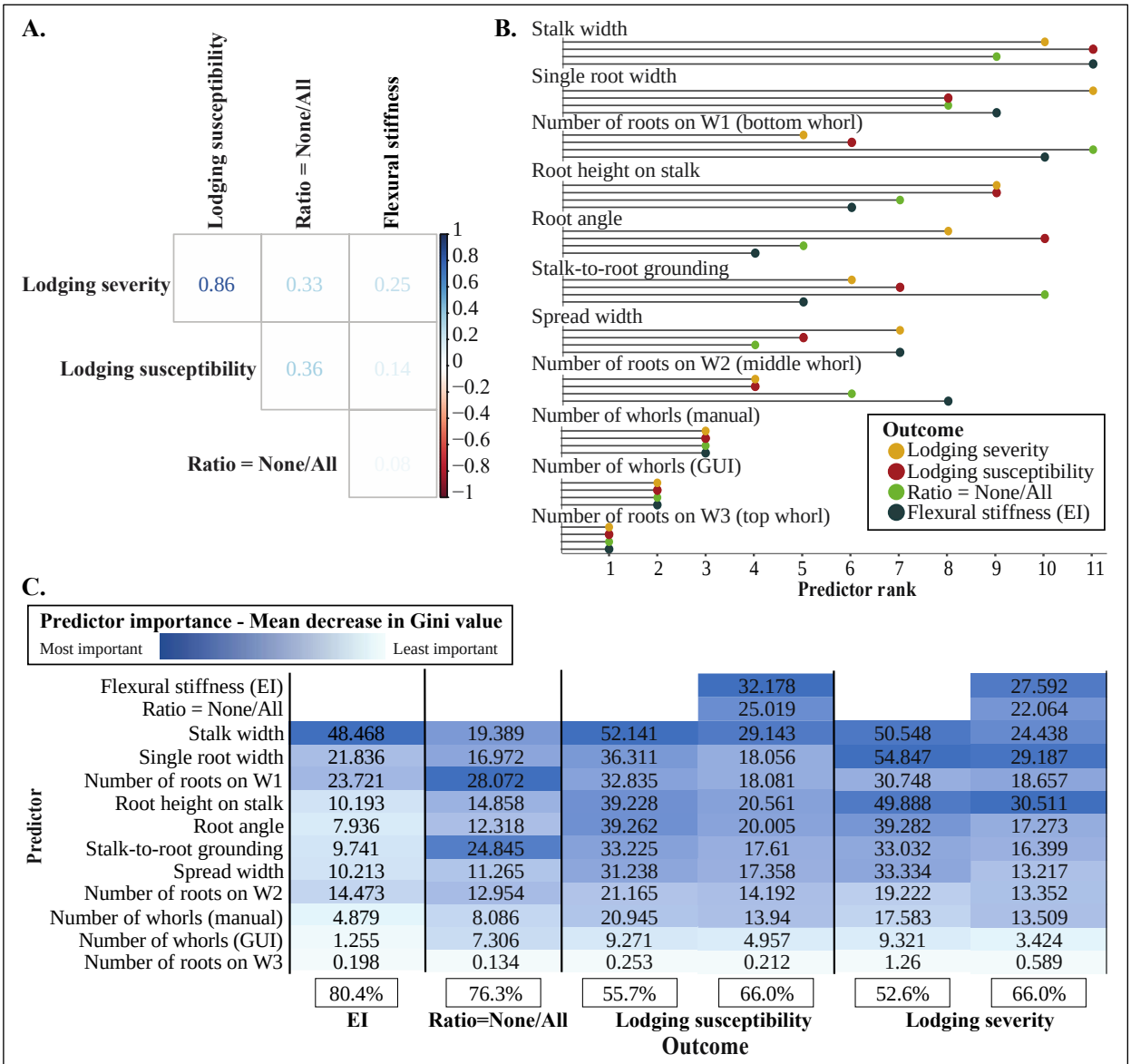

Figure 5. Multiple brace root phenotypes are associated with root lodging and anchorage. (A) There is a moderate correlation between root lodging (susceptibility and severity) and mechanical phenotypes (EI and the none/all ratio). (B) The predictors were ranked for each of the random forest models from 1-11, with 1 indicating the least important predictor in the model and 11 indicating the most important predictor in the model. The predictor ranks are similar across all of the models. (C) The predictor importance for each of the random forest models was determined by the mean decrease in Gini value. A darker shade of blue indicates that the corresponding predictor had a higher mean decrease in Gini value and thus was more important in the decision tree, whereas a lighter shade of blue/white indicates that the corresponding predictor had a lower mean decrease in Gini value and thus was less important. Predictors are ordered based on the relative importance as determined in (B). Boxed percentages indicate the prediction accuracy for the corresponding model.

random forest models, the mean decrease in Gini value can be used to assess the relative importance of each predictor in the decision tree. A higher Gini value indicates a greater influence on the decision tree and thus a more important predictor. For models that used only brace root phenotypes as predictors, the predictor ranks were comparable with stalk width ranking

consistently high and the number of roots on whorl 3 ranking consistently low (**Figure 5B**). The model that predicted stalk flexural stiffness was primarily influenced by stalk width (**Figure 5C**), which is consistent with a moderate correlation between these measures (**Table 1**) and previous reports linking stalk geometry with biomechanics (Robertson et al., 2017). In contrast, there are multiple predictors with similar influence on the brace root contribution (None/All ratio) and root lodging (susceptibility or severity) (**Figure 5C**). The influence of multiple phenotypes on prediction accuracy is consistent with the low correlations (**Table 1**) and the inconsistent phenotypes identified as associated with root lodging in previous studies (Liu et al., 2012; Sharma and Carena, 2016).

For root lodging models that included mechanical phenotypes as predictors, these predictors became equally influential as the brace root phenotypes (**Figure 5C**). Additionally, although the inclusion of plant height only improved the prediction accuracy of one model (outcome=root lodging susceptibility, predictors=brace root phenotypes, **Table 2**), plant height universally became the most important predictor for all decision trees (**Figure S9**). The lack of additional prediction accuracy from plant height in most models supports a link with brace root phenotypes and can be attributed to the opposing effects of these traits on root lodging. Together, these data show that the contribution of multiple brace root phenotypes is important for limiting root lodging and highlights the importance of uncoupling plant height and root system traits for future plant improvement.

Discussion

This study was motivated by a limited understanding of how brace root phenotypes contribute to root lodging resistance and plant anchorage. To address this limitation, data were integrated from a natural lodging event with measures of anchorage and brace root phenotypes. A robust workflow was developed to extract brace root phenotypes from a population of maize inbred lines. In linking brace root phenotypes to root lodging and anchorage, we confirmed that the number of brace root whorls in the ground is important for both outcomes. However, additional brace root phenotypes were identified that are more important in predicting root lodging and anchorage. The same phenotypes drive prediction accuracy for both natural root lodging and anchorage measures. Collectively, the data show brace root phenotypes that establish a wider base and thus increase stability are important in root lodging resistance and anchorage. These results highlight the importance of a multi-trait approach for understanding root lodging resistance.

Plant anchorage is an outcome of both above and below ground root systems. Integrating root lodging data with anchorage measurements, shows that genotypes with a lower contribution of brace roots to anchorage are more likely to root lodge. Surprisingly, this result demonstrates that brace roots are the primary contributor to crop anchorage.

The Green Revolution succeeded in reducing small grain crop lodging through a reduction in plant height. Here, when plant height was included a predictor, it became the most important predictor for all models. Generally, genotypes classified as root lodging resistant were shorter than genotypes that were classified as root lodging susceptible. However, the correlation was moderate ($r = 0.31$; **Table 1**), which indicates that plant height is not the only factor influencing root lodging. Interestingly, the inclusion of plant height did not always increase the overall model prediction

accuracy (**Table 2**), which suggests that the influence of plant height in the model was already captured by brace root phenotypes. We previously described the genetic linkage between plant height and brace root phenotypes (Hostetler et al., 2021), which is consistent with this outcome. Thus, future efforts to breed for root lodging resistance should consider decoupling brace roots from plant height to increase anchorage and root lodging resistance.

Acknowledgements

We thank members of the Sparks lab Sarah Blizard, and Noah Ouslander for assistance in mechanical testing. We thank Dr. Rajdeep Khangura (Purdue University) and Dr. Brandon Sinn (Otterbein University) for input in data analysis. We thank Dr. Jason Wallace (University of Georgia) for assistance in updating the root tagging pipeline to Python3. We thank members of the Vertically Integrated Projects course for beta-testing and debugging of the root tagging pipeline. We thank Teclemariam Weldekidan, Dr. Brian Dilkes (Purdue University), Dr. Colleen Drapek (Sainsbury Lab Cambridge), Dr. Anjali Iyer-Pascuzzi (Purdue University), Dr. Rajdeep Khangura (Purdue University), and Dr. Kevin Lehner (Colorado State University) for reviewing this manuscript and providing feedback. This work was supported by a Delaware Center for Advanced Technology grant and a University of Delaware Research Foundation (UDRF) award to EES.

Author Contributions

JWR, LE, AS, and EES collected data. ANH and EES analyzed data. WC, AS and HGT developed the semi-automated root phenotyping workflow. DDS provided DARLING devices and trained operators in their use. All authors contributed to the writing and editing of the manuscript.

Literature Cited

Berry, P. M., M. Sterling, J. H. Spink, C. J. Baker, R. Sylvester-Bradley, S. J. Mooney, A. R. Tams, and A. R. Ennos. 2004. Understanding and reducing lodging in cereals. Advances in Agronomy, 217–271. Elsevier.

Blizard, S., and E. E. Sparks. 2020. Maize Nodal Roots. Annual Plant Reviews online, 281–304. American Cancer Society.

Brune, P. F., A. Baumgarten, S. J. McKay, F. Technow, and J. J. Podhiny. 2018. A biomechanical model for maize root lodging. *Plant and Soil* 422: 397–408.

Carter, P. R., and K. D. Hudelson. 1988. Influence of simulated wind lodging on corn growth and grain yield. *Journal of Production Agriculture* 1: 295–299.

Chifman, J., and L. Kubatko. 2015. Identifiability of the unrooted species tree topology under the coalescent model with time-reversible substitution processes, site-specific rate variation, and invariable sites. *Journal of Theoretical Biology* 374: 35–47.

Chifman, J., and L. Kubatko. 2014. Quartet Inference from SNP Data Under the Coalescent Model. *Bioinformatics* 30: 3317–3324.

Cook, D. D., W. de la Chapelle, T.-C. Lin, S. Y. Lee, W. Sun, and D. J. Robertson. 2019. DARLING: a device for assessing resistance to lodging in grain crops. *Plant methods* 15: 102.

Das, A., H. Schneider, J. Burridge, A. K. M. Ascanio, T. Wojciechowski, C. N. Topp, J. P. Lynch, et al. 2015. Digital imaging of root traits (DIRT): a high-throughput computing and collaboration platform for field-based root phenomics. *Plant Methods* 11: 51.

Dhugga, K. S. 2007. Maize Biomass Yield and Composition for Biofuels. *Crop Science* 47: 2211–2227.

Erndwein, L., D. D. Cook, D. J. Robertson, and E. E. Sparks. 2020. Field-based mechanical phenotyping of cereal crops to assess lodging resistance. *Applications in Plant Sciences* 8: e11382.

Farkhari, M., A. Krivanek, Y. Xu, T. Rong, M. R. Naghavi, B. Y. Samadi, and Y. Lu. 2013. Root-lodging resistance in maize as an example for high-throughput genetic mapping via single nucleotide polymorphism-based selective genotyping. *Plant Breeding* 132: 90–98.

Flint-Garcia, S. A., C. Jampatong, L. L. Darrah, and M. D. McMullen. 2003. Quantitative Trait Locus Analysis of Stalk Strength in Four Maize Populations. *Crop Science* 43: 13–22.

Holland, J. B., W. E. Nyquist, and C. T. Cervantes-Martínez. 2002. Estimating and Interpreting Heritability for Plant Breeding: An Update. Plant Breeding Reviews, 9–112. John Wiley & Sons, Ltd.

Hoppe, D. C., M. E. McCully, and C. L. Wenzel. 1986. The nodal roots of Zea: their development in relation to structural features of the stem. *Canadian Journal of Botany* 64: 2524–2537.

Hostetler, A. N., R. S. Khangura, B. P. Dilkes, and E. E. Sparks. 2021. Bracing for sustainable agriculture: the development and function of brace roots in members of Poaceae. *Current Opinion in Plant Biology* 59: 101985.

Kassambara, A., and F. Mundt. 2020. factoextra: Extract and Visualize the Results of Multivariate Data Analyses.

Kuhn, M., and H. Wickham. 2020. Tidymodels: a collection of packages for modeling and machine learning using tidyverse principles.

Liu, S., F. Song, F. Liu, X. Zhu, and H. Xu. 2012. Effect of planting density on root lodging resistance and its relationship to nodal root growth characteristics in maize (Zea mays L.). *Journal of Agricultural Science* 4: 182.

Mangiafico, S. 2021. rcompanion: Functions to Support Extension Education Program Evaluation.

Menze, B. H., B. M. Kelm, R. Masuch, U. Himmelreich, P. Bachert, W. Petrich, and F. A. Hamprecht. 2009. A comparison of random forest and its Gini importance with standard chemometric methods for the feature selection and classification of spectral data. *BMC Bioinformatics* 10: 213.

R Core Team. 2013. R: A language and enviornment for satistical computing. R Foundation for Statistical Computing, Vienna, Austria.

Rajkumara, S. 2008. Lodging in cereals – a review. *Agricultural Reviews* 29: 55–60.

Reneau, J. W., R. S. Khangura, A. Stager, L. Erndwein, T. Weldekidan, D. D. Cook, B. P. Dilkes, and E. E. Sparks. 2020. Maize brace roots provide stalk anchorage. *Plant Direct* 4: e00284.

Robertson, D. J., M. Julias, S. Y. Lee, and D. D. Cook. 2017. Maize Stalk Lodging: Morphological Determinants of Stalk Strength. *Crop Science* 57: 926–934.

Salungyu, J., S. Thaitad, A. Bucksch, J. Kengkanna, and P. J. Saengwilai. 2020. From lab to field: Open tools facilitating the translation of maize root traits. *Field Crops Research* 255: 107872.

Sanguineti, M. C., M. Giuliani, G. Govi, R. Tuberosa, and P. Landi. 1998. Root and shoot traits of maize inbred lines grown in the field and in hydroponic culture and their relationships with root lodging. *Maydica* 43: 211–216.

Schliep, K., K. Hechenbichler, and A. Lizee. 2016. kknn: Weighted k-Nearest Neighbors.

Sharma, S., and M. J. Carena. 2016. BRACE: A Method for High Throughput Maize Phenotyping of Root Traits for Short-Season Drought Tolerance. *Crop Science* 56: 2996–3004.

Shi, J., B. J. Drummond, J. E. Habben, N. Brugire, B. P. Weers, S. M. Hakimi, H. R. Lafitte, et al. 2019. Ectopic expression of ARGOS8 reveals a role for ethylene in root-lodging resistance in maize. *The Plant Journal* 97: 378–390.

Stamp, P., and C. Kiel. 1992. Root morphology of maize and its relationship to root lodging. *Journal of Agronomy and Crop Science* 168: 113–118.

Thompson, D. L. 1972. Recurrent Selection for Lodging Susceptibility and Resistance in Corn1. *Crop Science* 12: cropsci1972.0011183X001200050023x.

Tirado, S. B., C. N. Hirsch, and N. M. Springer. 2020. Utilizing Temporal Measurements from UAVs to Assess Root Lodging in Maize and its Impact on Productivity. Plant Biology.

Trachsel, S., S. M. Kaeppler, K. M. Brown, and J. P. Lynch. 2011. Shovelomics: high throughput phenotyping of maize (Zea mays L.) root architecture in the field. *Plant and Soil* 341: 75–87.

Wascher, M., and L. Kubatko. 2021. Consistency of SVDQuartets and Maximum Likelihood for Coalescent-Based Species Tree Estimation. *Systematic Biology* 70: 33–48.

Wei, T., and V. Simko. 2017. R package ‘corrplot’: Visualization of a Correlation Matrix.

Wickham, H. 2016. ggplot2: Elegant Graphics for Data Analysis. R Foundation for Statistical Computing, Verlag, New York.

Wickham, H., M. Averick, J. Bryan, W. Chang, L. McGowan, R. François, G. Grolemund, et al. 2019. Welcome to the Tidyverse. *Journal of Open Source Software* 4: 1686.

Wright, M. N., and A. Ziegler. 2017. **ranger** : A Fast Implementation of Random Forests for High Dimensional Data in *C++* and *R*. *Journal of Statistical Software* 77.

Zhan, A., J. Liu, S. Yue, X. Chen, S. Li, and A. Bucksch. 2019. Architectural and anatomical responses of maize roots to agronomic practices in a semi-arid environment. *Journal of Plant Nutrition and Soil Science* 182: 751–762.

Zhang, Q., F. A. Pettolino, K. S. Dhugga, J. A. Rafalski, S. Tingey, J. Taylor, N. J. Shirley, et al. 2011. Cell Wall Modifications in Maize Pulvini in Response to Gravitational Stress. *Plant Physiology* 156: 2155–2171.

Tables

Table 1. Individual phenotype correlations with root lodging and mechanical phenotypes. A Pearson correlation was run on genotypic level phenotypes, root lodging susceptibility, root lodging severity, stalk flexural stiffness (EI), and the None/All ratio. Data represent correlation r values.

	2020		**2018**		**2019**	
	Lodging susceptibility	**Lodging severity**	**EI**	**Ratio (None/All)**	**EI**	**Ratio (None/All)**
Number of roots on W1	0.091	0.078	0.306	-0.024	0.403	0.106
Number of roots on W2	-0.286	-0.178	0.191	-0.219	0.368	-0.199
Number of roots on W3	-0.100	-0.050	0.213	-0.017	0.065	0.081
Single root width	-0.064	0.024	0.012	0.024	0.034	-0.211
Stalk width	0.090	0.101	0.424	0.053	0.567	0.265
Height of whorl	0.125	0.068	0.138	-0.040	0.260	-0.017
Stalk to root grounding	-0.193	-0.124	-0.026	-0.259	0.194	-0.370
Root angle	-0.282	-0.159	-0.170	-0.176	-0.151	-0.358
Spread width	-0.174	-0.104	0.041	-0.243	0.278	-0.318
Number of whorls in ground (GUI)	-0.238	-0.051	0.092	-0.121	0.288	-0.185
Number of whorls in ground (manual)	-0.433	-0.364	0.269	-0.108	0.247	-0.410
Plant height	0.313	0.452	0.450	-0.397	0.421	-0.233

Table 2. Prediction accuracy of random forest models. Random forest models were used to determine the prediction accuracy of root lodging (susceptibility and severity) and mechanical phenotypes (stalk flexural stiffness and the None/All ratio) with variable predictors. The average prediction accuracy and Receiver Operating Characteristic (ROC) Area Under the Curve (AUC) values were extracted from models and varied depending on predictors. Models were run either on genotypic averages for outcomes or for individual paired plant data. The predictors included in each model are indicated with an X.

Predictors			**Outcome**		**Result**	
Phenotypes	Height	Biomechanics	Metric	Genotypic or Paired	Accuracy	ROC
X			Lodging Suscept.	Genotypic	0.557	0.738
X	X		Lodging Suscept.	Genotypic	0.680	0.814
X			Lodging Severity	Genotypic	0.526	0.659
X	X		Lodging Severity	Genotypic	0.557	0.755
X			Flexural Stiffness	Genotypic	0.804	0.581
X	X		Flexural Stiffness	Genotypic	0.825	0.829
X			Flexural Stiffness	Paired	0.753	0.818
X	X		Flexural Stiffness	Paired	0.784	0.833
X			Ratio (None/All)	Genotypic	0.763	0.792
X	X		Ratio (None/All)	Genotypic	0.784	0.862
X			Ratio (None/All)	Paired	0.670	0.644
X	X		Ratio (None/All)	Paired	0.670	0.664
X		X	Lodging Suscept.	Genotypic	0.660	0.755
X	X	X	Lodging Suscept.	Genotypic	0.680	0.815
X		X	Lodging Severity	Genotypic	0.660	0.732
X	X	X	Lodging Severity	Genotypic	0.639	0.819

Supplementary Data

Figure S1. A ground-based brace root phenotyping robot (BRobot) was used for image capture. BRobot is a modified Superdroid LT2 Tracked ATR Robot Platform with a custom controller. The red arrow highlights the side-mounted FLIR 3.2 MP Color Blackfly camera that captures images.

Figure S2. A semi-automated root tagging workflow was developed to optimize image processing. After RGB images are acquired, a python script (*main.py*) launches the root tagging graphical user interface (GUI). A tag of known size (0.5 inches) was placed on the stem prior to image acquisition for scale. First, the tag is selected for a pixel (px) scale, then each additional screen will prompt the user to click and/or record/identify specific regions in the image. The red dots shown on the image highlight the following phenotypes that have been tagged: 1) the number of pixels within a 0.5-inch region, 2) the stalk width, and 3) the single root width. The purple dots shown on the image highlight the right triangle that is used to identify the following phenotypes: 1) the height of the whorl, 2) the stalk-to-root grounding, and 3) the root angle. The number of roots within each whorl was counted and typed into the white boxes (shown on the left). This records the total number of roots per whorl and the number of whorls in the ground. After recording or identifying phenotypes, the user will hit "enter." After all phenotypes have been recorded, the user will hit "Next" (red bar on the right of the screen) to begin the next image. After completing all images, a python script (*process_rootpixel_data.py*) is used to convert pixel data to scaled phenotype data. All data is exported to a .csv file for processing and analysis.

Figure S3. Phenotypes extracted from left and right images were highly correlated. Left and right images (labeled A and B) were acquired for each plant and phenotypes were extracted from images with the root tagging GUI. A Pearson correlation analysis was run to determine the precision of our root tagging GUI. Cells highlighted in yellow indicate the same phenotype from both sides of the plant.

Figure S4. Root lodging is not monophyletic. A species tree was generated for 41 of the 52 maize inbred genotypes included in this study. Genotype names are color coded according to their assigned subpopulation information [Flint-Garcia et al (2005) and Liu et al (2003)]. If all genotypes within a clade are from the same subpopulation, branches are solid and colored with the respective subpopulation. Branches are dotted if the clade includes genotypes from more than one subpopulation. Genotypes were identified as lodging resistant or variable per Figure 2. The assigned lodging classification is illustrated to the right of the genotype with a circle or square. Clades where all genotypes within the clade are a part of a single lodging classification are highlighted with the corresponding shape at the node.

Figure S5. Root lodging resistant genotypes had more brace root whorls in the ground. Images were acquired with BRobot one day before Tropical Storm Isaias. From the RGB images, the number of brace root whorls that entered the ground was extracted. Genotypes were classified as lodging resistant or variable according to Figure 2. Genotypes that were root lodging resistant had more brace root whorls in the ground compared to those that were root lodging susceptible ($p<0.05$).

Figure S6. Root lodging was not related to field position. Winds from the West and North-West induced root lodging. (A) Plots were colored according to the susceptibility of root lodging within each plot. Plots with 100% root lodging were highlighted with white, whereas plots that had 0% root lodging were highlighted with dark red. (B) Plots were colored according to the average severity score within the plot. Plots that are highlighted in white are plots where plants were on the ground (90-degree displacement), whereas plots that are highlighted in dark red are plots where plants remained vertical (lack of root lodging). (A-B) Plots with a grid overlaid indicate plots that did not germinate.

Figure S7. Plant phenotypes vary among genotypes. The following phenotypes vary among genotypes: (A) The number of roots on whorl 1 (the whorl closest to the ground, bottom whorl), (B) the number of roots on whorl 2 (middle whorl), (C) the number of roots on whorl 3 (top whorl), (D) the single root width, (E) the stalk width, (F) the root height on stalk, (G) the stalk-to-root grounding, (H) the root angle, (I) the spread width, (J) the number of whorls in the ground, quantified from the GUI, (K) the number of whorls in the ground, quantified manually, and (L) plant height. (A-L) Genotypes are ordered by root lodging classification as in Figure 2. The color of each dot illustrates the replicate plot where the phenotype data is from. Outliers are outlined in black.

Figure S8. Brace root phenotypes are correlated with each other. A Pearson correlation analysis shows which phenotypes are highly correlated.

Figure S9. The inclusion of plant height does not increase model prediction accuracy. A random forest model was generated to predict stalk flexural stiffness, the None/All ratio, root lodging susceptibility, and root lodging severity. For each of the models generated, predictors with a higher mean decrease in Gini value were more important compared to those with a lower mean decrease in Gini value. A darker shade of blue indicated predictors that were more important, whereas a lighter shade of blue/white indicated predictors that were less important in successfully predicting the outcome. Although there was not an increase in model accuracy, plant height became the most important predictor.

Table S1. List of 52 maize inbred genotypes with assigned subpopulation information. The subpopulation information for each of the 52 maize inbred genotypes included in this study was identified in Flint-Garcia et al (2005) and Liu et al (2003). Genotypes with missing information are denoted with a (*).

Table S2. Temperature, rainfall, and wind speed summaries for the 2018, 2019, and 2020 field seasons. For the duration of this study, the average temperature (degrees F), total rainfall (in), and average wind speeds (mph) were included for each of the months in the 2018, 2019, and 2020 field seasons. Additional weather data can be found at the Delaware Environmental Observing System (http://www.deos.udel.edu) and selecting the Newark, DE-Ag Farm station.

Table S3. Environmental Conditions Summary for Tropical Storm Isaias. The following 24-hour weather summary for August 04, 2020 was collected from the DEOS for the Newark, DE Agriculture Farm station. The Newark, DE Agricultural Farm Station is located at 39° 40' N and

75° 45' W at an elevation of 106 ft. Additional data can be viewed at: http://www.deos.udel.edu and selecting the Newark, DE-Ag Farm station.

Table S4. Heritability estimates for plant phenotype data, root lodging data, and mechanical phenotypes data. Broad-sense heritability (H^2) was estimated for plant phenotype data, root lodging data (susceptibility and severity), and mechanical phenotypes (stalk flexural stiffness (EI) and the none/all ratio).

Table S5. Descriptions of plant phenotype, root lodging, and mechanical phenotypes data. The phenotype name, unit of measurement, and phenotype description was included for each of the phenotypes quantified and examined within this study.

Table S6. Analysis of variance (ANOVA) results for plant phenotype data. A one-way ANOVA was run for each of the plant phenotypes included in this study with genotype as the independent variable and the corresponding plant phenotype as the dependent variable. With the exception of stalk width, all of the phenotypes were transformed with a Tukey ladder of powers transformation prior to running the ANOVA to meet the normality assumption. $p \leq 0.001$ (***); $p \leq 0.01$ (**); $p \leq 0.05$ (*)

Table S7. Pairwise comparisons for each of the 2019 phenotypes. A post-hoc Tukey's Honest Significant Difference (HSD) test was used to determine genotypes that were significantly different for each of the phenotypes measured. Genotypes that share a letter for a single phenotype indicate genotypes that are not significantly different, whereas genotypes that do not share a letter are significantly different. The p-value was assessed at ≤ 0.05.

Table S8. Summary statistics for each of the 11 dimensions from a principal component analysis (PCA). A standard deviation and proportion of variance were extracted for each of the 11 dimensions of the PCA. Within the first two dimensions 43.60% of the variance was explained and within seven dimensions more than 90% of the variance was explained.

Table S9. Variance contributions for each of the 11 dimensions from a principal component analysis (PCA). The contribution of each phenotype for dimensions 1-11 was extracted from the PCA.

Table S10. Analysis of variance (ANOVA) results for mechanical phenotypes. A two-way ANOVA was run for stalk flexural stiffness (EI) and the none/all ratio with genotype and year included as the independent variables. Prior to running the ANOVA, a Tukey ladder of powers transformation was applied to the stalk flexural stiffness data to meet the normality assumption. The stalk flexural stiffness varied among genotypes and years ($p<0.001$ for both), whereas the none/all ratio only varied among genotypes ($p<0.001$) and not years ($p>0.05$).

Table S11. Pairwise comparisons for 2018 and 2019 mechanical phenotypes. A post-hoc Tukey's Honest Significant Difference (HSD) test was used to determine genotypes that were significantly different for flexural stiffness (EI) and the none/all ratio. Genotypes that share a letter for stalk flexural stiffness or the none/all ratio indicate genotypes that are not significantly

different, whereas genotypes that do not share a letter are significantly different. The p-value was assessed at ≤ 0.05.